Multi-Source Cooperation with Full-Diversity Spectral-Efficiency and Controllable-Complexity

Alejandro Ribeiro, Renqiu Wang, and Georgios B. Giannakis

***Abstract*— A general framework is developed for multi-source cooperation (MSC) protocols to improve diversity and spectral efficiency relative to repetition based alternatives that rely on single-source cooperation. The novel protocols are flexible to balance tradeoffs among diversity, spectral efficiency and decoding-complexity. Users are grouped in clusters and follow a two-phase MSC protocol which involves time division multiple access (TDMA) to separate users within a cluster, and code division multiple access (CDMA) used to separate clusters. An attractive protocol under the general MSC framework relies on distributed complex field coding (DCFC) to enable diversity order equal to the number of users per cluster. Cluster separation based on orthonormal spreading sequences leads to spectral efficiency $1/2$. When the number of clusters exceeds the amount of spreading, spectral efficiency can be enhanced without sacrificing diversity, at the expense of controllable increase in complexity. Simulations corroborate our analytical claims.**

***Index Terms*—**

I. Introduction

IN WIRELESS communications, "good performance" at the physical layer is quantified by low error rate, high spectral efficiency and low complexity. On the other hand, multiplicative fading induced by the propagation environment and additive noise effects at the receiving end, render it impossible to optimize one metric without sacrificing the others. A universal system design should, therefore, be flexible to tradeoff among error performance, spectral efficiency and complexity.

Error probability over wireless Rayleigh fading channels is inversely proportional to the link signal-to-noise ratio (SNR), i.e., $P_e \propto \gamma^{-1}$; that is to be contrasted with additive white Gaussian noise (AWGN) channels where the same dependence is exponential, i.e., $P_e \propto \mathrm{e}^{-\gamma^2}$. This gap is closed with diversity techniques whereby non-redundant copies of the information bearing signal are coherently combined at the receiver. A pertinent definition when analyzing diversity enabling protocols is the diversity order

$$\eta := \lim_{\gamma\to\infty} \frac{\log[P_e(\gamma)]}{\log(\gamma)}. \tag{1}$$

Manuscript received February 6, 2006; revised July 12, 2006. Part of the results in this paper appeared in [10]. This work was prepared through collaborative participation in the Communications and Networks Consortium sponsored by the U. S. Army Research Laboratory under the Collaborative Technology Alliance Program, Cooperative Agreement DAAD19-01-2-0011. The U.S. Government is authorized to reproduce and distribute reprints for Government purposes notwithstanding any copyright notation thereon.

The authors are with the Dept. of Electrical and Computer Engr., Univ. of Minnesota, 200 Union Street SE, Minneapolis, MN 55455 (e-mail: {aribeiro, renqiu, georgios}@ece.umn.edu).

Digital Object Identifier 10.1109/JSAC.2007.0702xx.

Cooperative diversity is a recently introduced fading countermeasure in which single-antenna terminals cooperate to effect a virtual distributed antenna array. Early cooperative approaches were mainly based on distributed repetition coding according to which cooperating users repeat or re-encode the information bearing message received from a single source to the destination by either amplifying-and-forwarding or regenerating operations [5], [11], [13], [14]. Unfortunately, the resultant increase in diversity comes at the price of spectral efficiency loss. This loss can be mitigated with the use of distributed space-time codes [6]. Additional spectral efficiency enhancements are also possible through pseudo-noise or multi-code spreading sequences [11]. However, in all these protocols, one cooperating user is typically limited to serve as relay of a single source only, even in the multi-source scenarios of [11] and [6].

A novel, so called multi-source cooperation (MSC) approach relying on joint coding of multiple sources was introduced in [15] to improve bandwidth efficiency and diversity order. A two-phase MSC system with distributed convolutional coding (DCC) was reported in [17], along with a simple design of interleavers to maximize the diversity order of simple error events. A distributed trellis coded modulation (DTCM) based MSC system approaching the bandwidth efficiency of a non-cooperative time division multiple access (TDMA) system was developed in [16]. Assuming slow block fading Rayleigh channels with binary transmission, the maximum achievable diversity order effected by error control coding (ECC) in MSC networks with K users is $\eta = \min(d_{\min}, \lfloor 1 + K(1 - R_c) \rfloor)$, where $d_{\min}$ and R_c denote respectively the minimum (free) distance and the ECC rate [16], [17].

However, viewing K transmitting users as a virtual antenna array suggests that the attainable diversity order could be as high as K. Clearly, if $R_c > 1/K$, then MSC with ECC cannot achieve this maximum diversity order. This is actually inherent to the diversity properties of ECC. On the other hand, complex field coding (CFC) applied to co-located (N_t, N_r) multi-antenna systems is known to achieve transmission rate of N_t symbols per channel use with diversity order as high as the product of the number of transmit-receive antennas, i.e., $\eta_{\max} = N_t N_r$ [7], [19]. This motivates adoption of distributed CFC (DCFC) in MSC networks to effect diversity order equal to the number of cooperating users K.

This paper introduces a general MSC framework with full-diversity, flexible spectral efficiency and controllable decoding complexity. Users are grouped in clusters that are separated with code division multiple access (CDMA). Within each cluster users cooperate to reach the access point (AP), imple-

menting MSC according to a two-phase TDMA protocol (Section II). The first contribution of the present work is to show that the diversity order of MSC over fading channels coincides with the diversity order when the links between cooperating users are error-free (Section II-A). As the latter can be thought as a single user transmission over multiple input - single output (MISO) channels, two implications of this result are: i) the diversity order of repetition coding is $\eta_{\rm RC} = 2$; and ii) the maximum diversity order of distributed ECC is $\eta_{\rm DECC} = \min(d_{\min}, \lfloor 1 + K(1 - R_c) \rfloor)$. The second contribution of this paper is to establish that DCFC-based MSC enables diversity order equal to the number of users, $\eta_{\rm DCFC} = K$ (Section II-B). We further address cluster separation and demonstrate that when the number of clusters is larger than the spreading gain, flexible MSC protocols emerge trading off spectral efficiency, error performance and complexity (Section III). While coding gain is affected in this under-spread case the diversity order is not, thus enabling MSC protocols to achieve full diversity at maximum spectral-efficiency equal to that of non-cooperative networks. By adjusting the number of cooperating users, MSC encoder, spreading gain and/or the number of clusters, our general MSC framework is flexible to tradeoff among spectral-efficiency, decoding complexity and diversity (Section IV). Simulations verify that error performance is improved at low or no spectral-efficiency loss (Section V). We conclude the paper in Section VI.

Notation: Throughout the paper, lower (upper) case boldface letters will stand for column vectors (matrices) with ^{T} standing for transposition, * for complex conjugation and $^{\mathcal{H}}$ for conjugate transposition. The canonical basis of $\mathbb{C}^N$ will be denoted as $\{\mathbf{e}_1, \ldots, \mathbf{e}_N\}$ so that the $N \times N$ identity matrix can be written as $\mathbf{I}_N := [\mathbf{e}_1, \ldots, \mathbf{e}_N]$. The all-one and all-zero vectors in $\mathbb{C}^N$ will be denoted as $\mathbf{1}_N := [1, \ldots, 1]^T$ and $\mathbf{0}_N := [0, \ldots, 0]^T$, respectively. Finally, $\mathrm{E}[\cdot]$ will stand for expectation.

II. Multi-source cooperation

Consider the cooperative multiple access (MA) setup of Fig. 1 in which the set of active users is divided into L clusters $\{\mathcal{U}_l\}_{l=1}^L$. In each cluster, K_l users $\{U_{lk}\}_{k=1}^{K_l}$ cooperate in transmitting symbol blocks $\mathbf{s}_{lk} := [s_{lk1}, \ldots, s_{lkN}]^T$ of size $N \times 1$ to the AP that we write as U_{00}. We assume that $\mathbf{s}_{lk}$ contains a cyclic redundancy check (CRC) code allowing detection of correctly received packets. We let $\mathbf{h}_{l_1k_1,l_2k_2} := h_{l_1k_1,l_2k_2}\mathbf{1}_N$ denote the block Rayleigh fading channel between users $U_{l_1k_1}$ and $U_{l_2k_2}$; and $\mathbf{h}_{lk} := h_{lk}\mathbf{1}_N$ the one between U_{lk} and the AP. We further assume that these channels are uncorrelated and adopt the convention $\mathbf{h}_{lk,lk} \equiv \mathbf{1}_N$. Let us postpone to Section III the issue of cluster separation and focus on the operation of a single cluster, for which we set $L = 1$ and drop the cluster subscript l to simplify notation.

Supposing that frame synchronization has been established, TDMA is used to separate users per cluster as depicted in Fig. 2. The MSC protocol consists of two phases each taking place over K slots. With symbol duration T_s, unit-energy pulse waveform $p(t)$ with non-zero support T_s and amplitude A, the

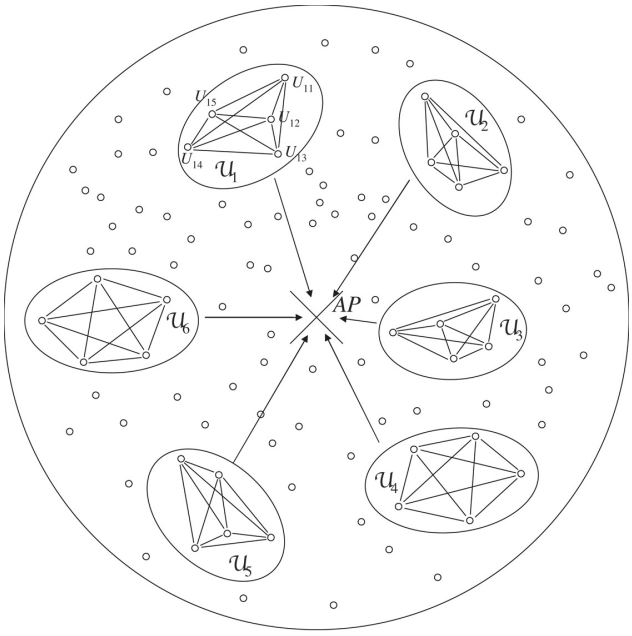

Fig. 1. Multiple access (MA) channel is divided in cooperating clusters.

waveform transmitted by source U_k during phase-1 is

$$x_k^{(1)}(t) = A \sum_{n=1}^{N} s_{kn} p\left[t - ((k-1)N + n)T_s\right], \quad t \in [0, KNT_s). \quad (2)$$

The waveforms $\{x_k^{(1)}(t)\}_{k=1}^K$ propagate through the shared wireless interface so that over a burst of KNT_s seconds each user in the cluster, say U_k, has available the waveform $y_k^{(1)}(t) = \sum_{j=1}^K h_{j,k}(t) x_j^{(1)}(t) + n(t)$, where $n(t)$ denotes AWGN with double-sided spectral density $N_0/2$. The waveform $y_k^{(1)}(t)$ is subsequently match filtered yielding samples $y_{k,jn} = \int_0^{T_s} y_k^{(1)}[t - ((j-1)N + n)T_s]p^*(t)dt$. Upon defining the aggregate $KN \times 1$ transmitted and received blocks $\mathbf{s} := [\mathbf{s}_1^T, \ldots, \mathbf{s}_K^T]^T$ and $\mathbf{y}_k^{(1)} := [y_{k,11}, \ldots, y_{k,1N}, y_{k,21}, \ldots, y_{k,KN}]^T$, the noise vector $\mathbf{n}_k^{(1)} := [n_{k,11}, \ldots, n_{k,KN}]^T$ and the diagonal channel matrix $\mathbf{D}_k^{(1)} := \mathrm{diag}(\mathbf{h}_{k,1}^T, \ldots, \mathbf{h}_{k,K}^T)$, the input-output relationship per user U_k during phase-1 is

$$\mathbf{y}_k^{(1)} = A\mathbf{D}_k^{(1)}\mathbf{s} + \mathbf{n}_k^{(1)}, \qquad k = 0, 1, \ldots, K, \quad (3)$$

where by convention $\mathbf{h}_{k,k} \equiv \mathbf{1}_N \ \forall k$, $n_{k,kn} \equiv 0$ for $n \in [1, N]$ and we recall that $\mathbf{y}_0^{(1)}$ corresponds to the received block at the AP. For future use, we note that the transmit SNR is $\gamma := A^2/N_0$ and the average SNR in the $U_k \to U_j$ link is $\gamma_{k,j} := (A^2/N_0)\mathrm{E}[h_{k,j}^2] = \gamma \mathrm{E}[h_{k,j}^2]$.

Notice that by the end of phase-1 every user has available information about the symbol blocks of all users in the cluster $\mathcal{U}$. User U_k ($k > 0$) estimates the joint block $\mathbf{s}$, with entries drawn from a signal constellation $\mathcal{S}$, using the maximum likelihood (ML) decoder [c.f. (3)]

$$\hat{\mathbf{s}}_k = \arg \min_{\mathbf{s} \in \mathcal{S}^N} \|\mathbf{y}_k^{(1)} - A\mathbf{D}_k^{(1)}\mathbf{s}\|. \quad (4)$$

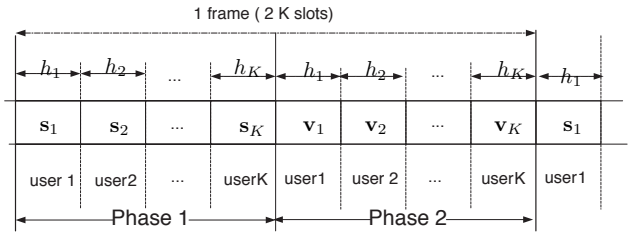

Fig. 2. TDMA structure of an MSC protocol for a cluster with K active users.

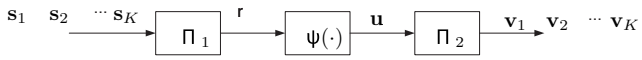

Fig. 3. Encoder and interleaving modules of each cooperating user.

If symbols in $\mathbf{s}$ are uncoded, then (4) amounts to symbol-by-symbol detection since $\mathbf{D}_k^{(1)}$ is diagonal; whereas if the individual blocks $\mathbf{s}_k$ are protected with ECC, then (4) implements block detection. Since not all users in $\mathcal{U}$ decode $\mathbf{s}$ correctly, we define the set of those that do as

$$\mathcal{D} := \{U_k \mid \hat{\mathbf{s}}_k = \mathbf{s}\} \subseteq \mathcal{U}. \tag{5}$$

Users in $\mathcal{D}$ proceed to phase-2, but before transmission they process $\mathbf{s}$ as shown in Fig. 3. The aggregate block $\mathbf{s}$ is fed to an interleaver, Π_1, yielding the vector $\mathbf{r} = \mathbf{\Pi}_1\mathbf{s}$. The interleaved block $\mathbf{r}$ is then encoded with a function $\psi(\cdot)$ to obtain $\mathbf{u} = \psi(\mathbf{r})$, which is subsequently fed to a second interleaver, Π_2, to obtain the block $\mathbf{v} = \mathbf{\Pi}_2\mathbf{u}$. This processing per user in $\mathcal{D}$ can be summarized as

$$\mathbf{v} = \mathbf{\Pi}_2\mathbf{u} = \mathbf{\Pi}_2\psi(\mathbf{r}) = \mathbf{\Pi}_2\psi(\mathbf{\Pi}_1\mathbf{s}). \tag{6}$$

Since all operations in (6) preserve dimensionality, we have that the blocks $\mathbf{v}, \mathbf{u}, \mathbf{r} \in \mathbb{C}^{NK\times 1}$, the matrices $\mathbf{\Pi}_1, \mathbf{\Pi}_2 \in \mathbb{C}^{NK\times NK}$ and the encoder $\psi : \mathbb{C}^{NK\times 1} \to \mathbb{C}^{NK\times 1}$.

Each user in $\mathcal{D}$ transmits again in a TDMA fashion an $N \times 1$ sub-block of the block $\mathbf{v} := [v_{11}, \ldots, v_{1N}, v_{21}, \ldots, v_{KN}]^T$. Specifically, U_k transmits the sub-block $\mathbf{v}_k := [v_{k1}, \ldots, v_{kN}]^T$ using the waveform

$$x_k^{(2)}(t) = A\sum_{n=1}^{N} v_{kn}\, p\left[t - ((k-1)N + n)T_s\right], \quad t \in [0, KNT_s). \tag{7}$$

The AP receives $x_k^{(2)}(t)$ from all users $U_k \in \mathcal{D}$ and nothing from the remaining users $U_k \notin \mathcal{D}$. To describe this reception, define the $N \times 1$ channel vector $\mathbf{h}_k^{(2)} := \mathbf{h}_k$, if $U_k \in \mathcal{D}$; and $\mathbf{h}_k^{(2)} := \mathbf{0}_N$, otherwise. Using this model, the block of samples at the matched filter output of the AP in phase-2 is given by

$$\mathbf{y}_0^{(2)} = A\mathbf{D}_0^{(2)}\mathbf{\Pi}_2\psi(\mathbf{\Pi}_1\mathbf{s}) + \mathbf{n}_0^{(2)}, \tag{8}$$

where $\mathbf{D}_0^{(2)} := \mathrm{diag}(\mathbf{h}_1^{(2)}, \ldots, \mathbf{h}_K^{(2)})$. The blocks $\mathbf{y}_0^{(1)}$ and $\mathbf{y}_0^{(2)}$ received in the two phases can be combined in the aggregate input-output relationship

$$\begin{bmatrix} \mathbf{y}_0^{(1)} \\ \mathbf{y}_0^{(2)} \end{bmatrix}_{2KN\times 1} = A\begin{bmatrix} \mathbf{D}_0^{(1)}\mathbf{s} \\ \mathbf{D}_0^{(2)}\mathbf{\Pi}_2\psi(\mathbf{\Pi}_1\mathbf{s}) \end{bmatrix} + \begin{bmatrix} \mathbf{n}_0^{(1)} \\ \mathbf{n}_0^{(2)} \end{bmatrix} \tag{9}$$

that the AP relies on to jointly decode $\mathbf{s}$. Note that all channels are assumed invariant over the duration of the two phases. Furthermore, since we transmit KN symbols in $2KN$ time slots, the spectral efficiency of single-cluster MSC is $\xi = 1/2$.

If all the diagonal entries of $\mathbf{D}_0^{(1)}$ and $\mathbf{D}_0^{(2)}$ were Rayleigh distributed, then (9) could be thought as the input-output relationship of a coded MISO system transmitting $\mathbf{s}$ and its encoded version over K antennas with only one antenna transmitting N symbol periods in a cyclic fashion. Equivalently, (9) could model an $1 \times K$ single input - multiple output (SIMO) channel with K receive antennas, or, a single antenna time-selective block fading channel with K degrees of freedom. In any event, the diversity order can be evaluated once the encoder $\psi(\cdot)$ has been specified. Having as elements the (Rayleigh) block fading channels $\mathbf{h}_k$ between U_k and the AP, $\mathbf{D}_0^{(1)}$ is Rayleigh distributed. However, the second phase equivalent channels $\mathbf{h}_k^{(2)}$ have a distribution that depends on the probability of successful decoding – recall that $\mathbf{h}_k^{(2)} := \mathbf{h}_k$, if $U_k \in \mathcal{D}$; and $\mathbf{h}_k^{(2)} := \mathbf{0}_N$, otherwise. While this distribution is not difficult to characterize it is certainly not Rayleigh; hence, $\mathbf{D}_0^{(2)}$ is not Rayleigh distributed either. We will prove later in Theorem 1 that even if $\mathbf{D}_0^{(2)}$ is not Rayleigh distributed the diversity order of MSC protocols coincides with the diversity order when $\mathbf{D}_0^{(2)}$ is Rayleigh distributed.

Defining a particular MSC protocol amounts to specifying the triplet $(\mathbf{\Pi}_2, \psi(\cdot), \mathbf{\Pi}_1)$ in (6). The diversity enabled by any MSC protocol is mainly determined by the encoder $\psi(\cdot)$; while the interleavers $\mathbf{\Pi}_1$ and $\mathbf{\Pi}_2$ distribute relayed symbols to different channels in order to effect the diversity order enabled by $\psi(\cdot)$. In this sense, the unifying framework presented in this section subsumes a number of existing cooperative protocols as special cases. Three of them are highlighted next.

[C1] **Distributed repetition coding:** Setting the permutation matrices $\mathbf{\Pi}_1 = \mathbf{\Pi}_2 = \mathbf{I}$ and selecting the encoder as

$$\begin{aligned}\psi_R(\mathbf{r}) = \psi_R(\mathbf{s}) &= \psi_R([\mathbf{s}_1^T, \ldots, \mathbf{s}_K^T]^T) \\ &:= [\mathbf{s}_2^T, \ldots, \mathbf{s}_K^T, \mathbf{s}_1^T]^T,\end{aligned} \tag{10}$$

reduces the input-output relationships (3) and (8) to those encountered with MSC based on repetition coding whereby U_k repeats U_{k-1}'s frame for $k \neq 1$ and U_1 repeats U_K's frame [14].

[C2] **Distributed ECC:** Let $\varphi(\cdot)$ be the function mapping a symbol vector over the *Galois field* $GF(m)$, to a channel codeword and $\varphi^{-1}(\cdot)$ the corresponding demapping function. Let also $\mathbf{P}$ denote the generator matrix of a channel encoder $\psi_P(\mathbf{r}) := \varphi(\mathbf{P}\varphi^{-1}(\mathbf{r}))$ with multiplication defined over $GF(m)$. If $\mathbf{P}$ generates a Reed-Solomon code, $\psi_P(\mathbf{r})$ specifies the MSC protocol in [15]; whereas if $\mathbf{P}$ generates a convolutional code, $\psi_P(\mathbf{r})$ gives rise to the DCC based MSC protocol in [17]. To effect the diversity, $\mathbf{\Pi}_1$ and $\mathbf{\Pi}_2$ have to be tailored for each chosen ECC [17]. Other channel codes, including distributed trellis coded modulation [16], are also possible choices.

[C3] **Distributed CFC:** Consider now the encoder $\psi_\Phi(\mathbf{r}) = \mathbf{\Phi}\mathbf{r}$, where $\mathbf{\Phi}$ is a block diagonal matrix with complex entries and multiplication is over the

complex field. This selection of $\psi(\cdot)$ corresponds to distributed complex field coding (DCFC) that we will elaborate on later in this section.

Remark 1 The set $\mathcal{D}$ of users that correctly decoded $\mathbf{s}$ does not need to be known to the cooperating users. This feature is important in practical deployment and can be readily verified by inspecting the encoder steps in (6) which clearly do not depend on $\mathcal{D}$.

A. Diversity Analysis

The diversity order η in (1) enabled by the generic MSC protocol we described so far depends on the encoder $\psi(\mathbf{r})$ in (6). Even though this precludes assessment of the diversity order without referring to a specific $\psi(\mathbf{r})$, we can obtain a general result by relating the MSC setup with an equivalent *single-user* transmission of $[\mathbf{s}^T, \mathbf{v}^T]^T$ (comprising the systematic and parity symbols) over a single-antenna block fading channel $\mathbf{D}_0^{(1)}$. If the links between cooperating users are error-free, then $\mathcal{D} \equiv \mathcal{U}$ and (8) becomes

$$\mathbf{y}_0^{(2)} = \mathbf{D}_0^{(1)} \mathbf{\Pi}_2 \psi(\mathbf{\Pi}_1 \mathbf{s}) + \mathbf{n}_0^{(2)}. \tag{11}$$

The AP can, therefore, decode $\mathbf{s}$ as if it were transmitted by a single user over a single time-selective fading channel. The only difference between (8) and (11) is that the channel matrix $\mathbf{D}_0^{(2)}$ in (8) is replaced by $\mathbf{D}_0^{(1)}$ in (11). From a statistical point of view, the only difference between these two models is the probability distribution of $\mathbf{D}_0^{(1)}$ and $\mathbf{D}_0^{(2)}$; from a practical perspective, we can think of (11) as the limiting case of (8) with perfect decoding in user-to-user links. Regardless of the interpretation, the important point is stated in the following theorem.

Theorem 1 *Let $\eta[\mathbf{\Pi}_2, \psi(\cdot), \mathbf{\Pi}_1]$ be the diversity order of the MSC protocol with input-output relations given by* (3) *and* (8). *Likewise, let $\beta[\mathbf{\Pi}_2, \psi(\cdot), \mathbf{\Pi}_1]$ be the diversity order of the equivalent single user protocol with input-output relations* (3) *and* (11). *Then, for any encoder $\psi(\cdot)$ and permutation matrices $\mathbf{\Pi}_1$, $\mathbf{\Pi}_2$, it holds that*

$$\eta[\mathbf{\Pi}_2, \psi(\cdot), \mathbf{\Pi}_1] = \beta[\mathbf{\Pi}_2, \psi(\cdot), \mathbf{\Pi}_1]. \tag{12}$$

To prove Theorem 1 we need two lemmas. In Lemma 1 we assess the diversity order conditioned on the set of decoders $\mathcal{D}$ (see Appendix A for the proof). In Lemma 2, we characterize the probability distribution of $\mathcal{D}$ as $\gamma \to \infty$ (see Appendix B for the proof).

Lemma 1 *If $\eta(\mathcal{D}) := \lim_{\gamma\to\infty} \log[P_e(\gamma|\mathcal{D})]/\log(\gamma)$ denotes the diversity order of the MSC protocol in Theorem 1 conditioned on the decoding set $\mathcal{D}$, then*

$$\eta(\mathcal{D}) \geq \max[0; \beta - (K - |\mathcal{D}|)], \tag{13}$$

where $|\mathcal{D}|$ is the cardinality of $\mathcal{D}$ and $\beta := \beta[\mathbf{\Pi}_2, \psi(\cdot), \mathbf{\Pi}_1]$.

Lemma 2 *The probability $\Pr(\mathcal{D})$ of the decoding set $\mathcal{D}$ is such that*

$$\lim_{\gamma\to\infty} \frac{\log[\Pr(\mathcal{D})]}{\log(\gamma)} = -(K - |\mathcal{D}|). \tag{14}$$

Lemma 1 establishes the intuitively expected result that the diversity order decreases by the number $K - |\mathcal{D}|$ of users who did not decode $\mathbf{s}$ correctly. However, Lemma 2 shows that as $\gamma \to \infty$ the probability of this event behaves precisely as $\gamma^{-(K-|\mathcal{D}|)}$. These two effects annihilate each other leading to Theorem 1 that we prove next.

Proof of Theorem 1: From the theorem of total probability $P_e(\gamma) = \sum_{\mathcal{D}} P_e(\mathcal{D}) \Pr(\mathcal{D})$, and thus

$$\begin{aligned} \eta &= -\lim_{\gamma\to\infty} \frac{\log\left[\sum_{\mathcal{D}} P_e(\mathcal{D}) \Pr(\mathcal{D})\right]}{\log(\gamma)} \\ &= -\min_{\mathcal{D}} \left\{ \lim_{\gamma\to\infty} \frac{\log\left[P_e(\mathcal{D}) \Pr(\mathcal{D})\right]}{\log(\gamma)} \right\}, \end{aligned} \tag{15}$$

where the second equality is a manifestation of the fact that the slowest term dominates the convergence ratio. This can be further separated as

$$\begin{aligned} \eta &= \min_{\mathcal{D}} \left\{ -\lim_{\gamma\to\infty} \frac{\log[P_e(\mathcal{D})]}{\log(\gamma)} - \lim_{\gamma\to\infty} \frac{\log[\Pr(\mathcal{D})]}{\log(\gamma)} \right\} \\ &= \min_{\mathcal{D}} \left\{ \eta(\mathcal{D}) - \lim_{\gamma\to\infty} \frac{\log[\Pr(\mathcal{D})]}{\log(\gamma)} \right\}. \end{aligned} \tag{16}$$

The first limit in (16) is given by Lemma 1 and the second by Lemma 2, based on which we obtain

$$\eta = \min_{\mathcal{D}} \{\max[0; \beta - (K - |\mathcal{D}|)] + (K - |\mathcal{D}|)\} = \beta \tag{17}$$

after substituting (13) and (14) into (16). □

The value of Theorem 1 is twofold. On the one hand, it establishes that diversity results for MISO channels carry over to judiciously designed MSC protocols. In particular, two immediate implications of Theorem 1 are stated in the following corollaries.

Corollary 1 *Diversity order of the repetition coding based MSC protocol in* [C1] *is $\eta(\mathbf{I}, \psi_R(\cdot), \mathbf{I}) = 2$.*

Proof: For repetition coding, the equivalent single-user protocol described by (3)-(11) can be readily shown to correspond to an uncoded 2×1 MISO channel which is known to provide second-order diversity. □

Corollary 2 *For the MSC protocol based on distributed ECC in* [C2] *with minimum distance $d_{\min}$ and code rate R_c, there exist matrices $\mathbf{\Pi}_1(\mathbf{P})$ and $\mathbf{\Pi}_2(\mathbf{P})$ so that*

$$\eta[\mathbf{\Pi}_2(\mathbf{P}), \psi_P(\cdot), \mathbf{\Pi}_1(\mathbf{P})] = \min(d_{\min}, \lfloor 1 + K(1 - R_c) \rfloor). \tag{18}$$

Proof: The result in (18) holds true for a single-antenna time-selective block fading channel; see e.g., [9, Ch.14]. It is thus true for MSC with distributed ECC because of Theorem 1. □

On the other hand, Theorem 1 establishes that designing good encoders $\psi(\cdot)$ is equivalent to designing diversity-enabling codes for co-located multi-antenna transmitters with the advantage that the latter is a well-understood problem. An interesting observation in this regard is that since there are K uncorrelated Rayleigh channels in (11), the potential diversity order is K. MSC protocols based on distributed repetition

coding or distributed ECC fail to enable this diversity order. The solution in co-located multi-antenna systems is to use complex field coding (CFC) [19], which motivates exploring CFC possibilities in a distributed setup.

B. Distributed Complex Field Coding

While in principle any matrix $\mathbf{\Phi}$ with complex entries could be used, the diversity order enabled by the DCFC protocol in [C3] depends critically on the choice of $\mathbf{\Phi}$. To make this point clear, we start by specifying the permutation matrices $\mathbf{\Pi}_1$, $\mathbf{\Pi}_2$ as KN-dimensional periodic interleavers. Letting $\mathbf{e}_i$ denote the i^{th} element of the canonical basis of $\mathbb{C}^{KN}$, we select

$$\begin{aligned}\mathbf{\Pi}_1 = \mathbf{\Pi}_{KN} &:= [\mathbf{e}_1, \mathbf{e}_N, \ldots, \mathbf{e}_{(K-1)N+1}, \mathbf{e}_2, \mathbf{e}_{N+1}, \ldots, \mathbf{e}_{KN}],\\ \mathbf{\Pi}_2 = \mathbf{\Pi}_{NK} &:= [\mathbf{e}_1, \mathbf{e}_K, \ldots, \mathbf{e}_{(N-1)K+1}, \mathbf{e}_2, \mathbf{e}_{K+1}, \ldots, \mathbf{e}_{KN}].\end{aligned} \tag{19}$$

The period of $\mathbf{\Pi}_1 = \mathbf{\Pi}_{KN}$ is K and consequently it changes the ordering of $\mathbf{s}$ so that in $\mathbf{r} = \mathbf{\Pi}_1\mathbf{s}$, same symbol indices across users appear consecutively in $\mathbf{r} = [s_{11}, s_{21} \ldots, s_{K1}, s_{12}, \ldots, s_{KN}]^T$. Likewise, the period of $\mathbf{\Pi}_2 = \mathbf{\Pi}_{NK}$ is N, so that $\mathbf{\Pi}_2 = \mathbf{\Pi}_1^T = \mathbf{\Pi}_1^{-1}$.

The permutation matrix $\mathbf{\Pi}_1$ models the interleaver Π_1 shown in Fig. 4. Each terminal in $\mathcal{D}$ correctly decodes the N symbols of all users including its own symbols that are arranged in the K vectors $\mathbf{s}_k := [s_{1k}, \ldots, s_{Nk}]^T$, $k \in [1, K]$. These KN symbols are fed to the interleaver Π_1 which outputs the N vectors $\mathbf{r}_n := [s_{n1}, \ldots, s_{nK}]^T$, $n \in [1, N]$, that contain the n^{th} symbols of all K terminals. In matrix-vector form, this relation can be written as

$$[\mathbf{r}_1^T, \ldots, \mathbf{r}_N^T]^T := \mathbf{r} = \mathbf{\Pi}_1\mathbf{s} := \mathbf{\Pi}_1[\mathbf{s}_1^T, \ldots, \mathbf{s}_K^T]^T. \tag{20}$$

We consider the DCFC based MSC protocol in which each of these $\mathbf{r}_n$ blocks is CFC-encoded independently yielding the vectors $\mathbf{u}_n := \mathbf{\Theta}\mathbf{r}_n$, corresponding to the selection $\mathbf{\Phi} := \mathrm{diag}(\mathbf{\Theta}, \ldots, \mathbf{\Theta})$ in [C3]. These N vectors $\mathbf{u}_n := [v_{n1}, \ldots, v_{nK}]^T$, $n \in [1, N]$, are then fed to the interleaver Π_2 whose output consists of K vectors $\mathbf{v}_k := [v_{1k}, \ldots, v_{Nk}]^T$, $k \in [1, K]$, each containing the k^{th} element of all vectors $\mathbf{u}_n$, $n \in [1, N]$. Again, this can be written using matrix-vector notation as

$$[\mathbf{v}_1^T, \ldots, \mathbf{v}_K^T]^T := \mathbf{v} = \mathbf{\Pi}_2\mathbf{u} := \mathbf{\Pi}_2[\mathbf{u}_1^T, \ldots, \mathbf{u}_N^T]^T. \tag{21}$$

User U_k transmits the vector $\mathbf{v}_k$ leading to the phase-2 input/output relationship (8). We then de-interleave the received blocks at the AP to obtain [c.f. (8)]

$$\mathbf{\Pi}_1\mathbf{y}_0^{(2)} = A(\mathbf{\Pi}_1\mathbf{D}_0^{(2)}\mathbf{\Pi}_2)\,\mathbf{\Phi}\mathbf{r} + \mathbf{\Pi}_1\mathbf{n}_0^{(2)}. \tag{22}$$

Interestingly, since $\mathbf{\Pi}_2 = \mathbf{\Pi}_1^{-1}$ we have $\mathbf{\Pi}_1\mathbf{D}_0^{(2)}\mathbf{\Pi}_2 = \mathrm{diag}(h_1^{(2)}, \ldots, h_K^{(2)}, \ldots, h_1^{(2)}, \ldots, h_K^{(2)})$. Thus, upon defining $\mathbf{y}_{0n}^{(2)} := [y_{n1}^{(2)}, \ldots, y_{nK}^{(2)}]^T$, $\mathbf{n}_{0n}^{(2)} := [n_{n1}^{(2)}, \ldots, n_{nK}^{(2)}]^T$ and $\mathbf{D}_{0n}^{(2)} := \mathrm{diag}(h_1^{(2)}, \ldots, h_K^{(2)})$; and recalling that $\mathbf{\Phi}$ is block diagonal, we can write

$$\mathbf{y}_{0n}^{(2)} = A\mathbf{D}_{0n}^{(2)}\mathbf{u}_n + \mathbf{n}_{0n}^{(2)} = A\mathbf{D}_{0n}^{(2)}\mathbf{\Theta}\mathbf{r}_n + \mathbf{n}_{0n}^{(2)}, \quad n \in [1, N]; \tag{23}$$

which amounts to separating (22) in N decoupled equations, each involving the $K \times 1$ vectors $\mathbf{r}_n$, $\mathbf{y}_{0n}^{(2)}$, and $\mathbf{n}_{0n}^{(2)}$ instead of the $KN \times 1$ vectors $\mathbf{r}$, $\mathbf{y}_0^{(2)}$, and $\mathbf{n}_0^{(2)}$.

If we finally combine $\mathbf{y}_{0n}^{(2)}$ in (23) with its counterpart $\mathbf{y}_{0n}^{(1)} := [y_{n1}^{(1)}, \ldots, y_{nK}^{(1)}]^T$ from (3) corresponding to the channel matrix $\mathbf{D}_{0n}^{(1)} := \mathrm{diag}(h_1 \ldots\ h_K)$, the ML decoder for a DCFC based MSC protocol is

$$\hat{\mathbf{r}}_n = \arg \min_{\mathbf{r}_n \in \mathcal{S}^K} \left\| \begin{bmatrix} \mathbf{y}_{0n}^{(1)} \\ \mathbf{y}_{0n}^{(2)} \end{bmatrix}_{2K\times 1} - A \begin{bmatrix} \mathbf{D}_{0n}^{(1)} \\ \mathbf{D}_{0n}^{(2)}\mathbf{\Theta} \end{bmatrix}_{2K\times K} \mathbf{r}_n \right\|. \tag{24}$$

It is worth stressing that DCFC decoding in (24) operates on blocks of K symbols. (Near)-ML decoders, such as the sphere decoder [4], [8], [20], can be used to obtain $\hat{\mathbf{s}}_n$ from (24) with polynomial average complexity (cubic for moderate size K and SNR [4]). Certainly, if only quadratic complexity can be afforded, zero forcing, minimum mean-squared error or decision-feedback equalizer options are available but they cannot guarantee to achieve the maximum possible diversity order.

The advantage of the formulation in (23) is that the CFC encoder $\mathbf{\Theta}$ operates on $K \times 1$ symbol blocks which reduces complexity considerably relative to a KN-symbol CFC encoder. Also, basic CFC results derived for co-located multi-antenna systems [19] can be directly applied to the distributed MSC setup. In particular, it is useful to recall the notion of maximum distance separable (MDS) matrices.

Definition 1 *A matrix $\mathbf{\Theta}$ is called MDS with respect to the constellation $\mathcal{S}$ if and only if for any two different symbols $\mathbf{r}_1 \neq \mathbf{r}_2 \in \mathcal{S}$, all the coordinates of $\mathbf{\Theta}\mathbf{r}_1$ and $\mathbf{\Theta}\mathbf{r}_2$ are different i.e., $[\mathbf{\Theta}\mathbf{r}_1]_i \neq [\mathbf{\Theta}\mathbf{r}_2]_i$, $\forall i$.*

The MDS property leads to the following corollary of Theorem 1.

Corollary 3 *If $\mathbf{\Theta}$ is MDS with respect to $\mathcal{S}$, the DCFC based MSC protocol in* [C3] *with $\mathbf{\Phi} = \mathrm{diag}(\mathbf{\Theta}, \ldots \mathbf{\Theta})$ and $\mathbf{\Pi}_1$, $\mathbf{\Pi}_2$ given by* (19) *enables diversity equal to the number of users; i.e.,*

$$\eta[\mathbf{\Pi}_2, \mathbf{\Phi}(\cdot), \mathbf{\Pi}_1] = K. \tag{25}$$

Proof: Because of Theorem 1 it suffices to show that $\beta[\mathbf{\Pi}_2, \mathbf{\Phi}(\cdot), \mathbf{\Pi}_1] = K$. Let $d_H(\mathbf{u}_{n1}, \mathbf{u}_{n2})$ be the Hamming distance between codewords $\mathbf{u}_{n1}$ and $\mathbf{u}_{n2}$. When $\mathbf{D}_{0n}^{(2)}$ is Rayleigh distributed, the diversity order is $\beta[\mathbf{\Pi}_2, \mathbf{\Phi}(\cdot), \mathbf{\Pi}_1] = \min_{\mathbf{u}_{n1}, \mathbf{u}_{n2}} d_H(\mathbf{u}_{n1}, \mathbf{u}_{n2})$ [7, Sec. 2.1.2]. The MDS property guarantees that $\min_{\mathbf{u}_{n1}, \mathbf{u}_{n2}}[d_H(\mathbf{u}_{n1}, \mathbf{u}_{n2})] = K$ for $\mathbf{u}_n = \mathbf{\Theta}\mathbf{r}_n$ and consequently $\beta[\mathbf{\Pi}_2, \mathbf{\Phi}(\cdot), \mathbf{\Pi}_1] = K$. □

Remark 2 Relative to repetition based single-source cooperation (SSC), the MSC protocol based on distributed ECC or CFC can also enhance coding gains because relay transmissions are coded across time and space. As each source in MSC is served by multiple cooperators, for the same spectral efficiency, even ECC based MSC can achieve higher diversity gains than SSC. And since each cooperator serves multiple sources simultaneously, for the same diversity order, MSC can offer higher spectral efficiency than SSC. With regards to the cooperative multi-user protocol in [11] which relies on the presence of idle users, the unifying MSC protocol here does not require idle users. However, if K_I idle users are available and willing to cooperate, the protocol here can also

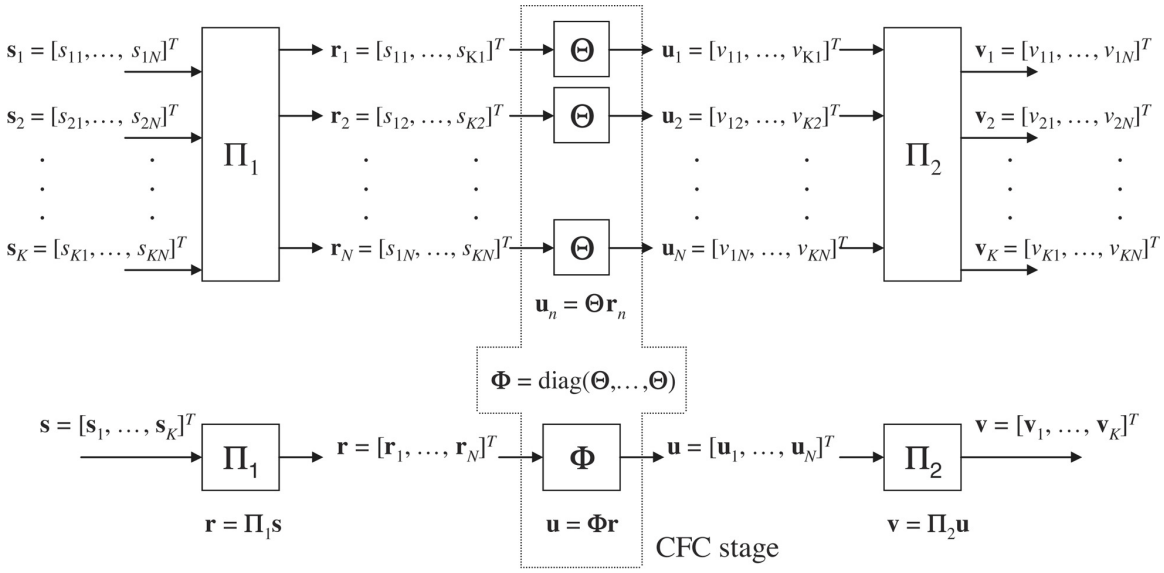

Fig. 4. Block diagram of DCFC per cooperating user.

take advantage of them to increase the diversity order up to $K + K_I$ per cluster.

III. Multi-cluster operation

Let us now return to the multi-cluster setting with $L > 1$ non-overlapping clusters communicating with the AP. Cluster separation can be accomplished with any multiple access (MA) scheme which in principle should not affect the properties of the DCFC based MSC protocol. However, it will turn out that MA with CFC can affect spectral efficiency of the MSC protocol.

Recall that $\mathbf{s}_{lk} := [s_{lk1}, \ldots, s_{lkN}]^T$ denotes the data packet of U_{lk} and $\mathbf{s}_l := [\mathbf{s}_{l1}^T, \ldots, \mathbf{s}_{lK}^T]^T$ the l^{th} cluster's aggregate block[1]. To separate clusters at the AP we rely on CDMA with spreading code signatures $\{c_l(t)\}_{l=1}^L$. To this end, the waveform transmitted by U_{lk} is

$$x_{lk}^{(1)}(t) = A \sum_{n=1}^{N} s_{lkn} c_l[t - (N(k-1)+n)T_s], \quad t \in [0, kNT_s). \tag{26}$$

The correlation between $c_l(t)$ and $c_m(t)$ will be denoted as $\rho_{ml} := \int_0^{T_s} c_l(t) c_m(t) dt$ and arranged in the symmetric $L \times L$ matrix $\mathbf{R}$ with entries $[\mathbf{R}]_{ml} := \rho_{ml}$.

User U_{lk} receives the superposition of what the remaining $LK - 1$ users transmit, namely

$$y_{lk}^{(1)}(t) = \sum_{m=1}^{L} \sum_{j=1}^{K} h_{lk,mj}\, x_{mj}^{(1)}(t) + n_{lk}^{(1)}(t). \tag{27}$$

For notational simplicity, let us consider the waveform $y_{00}^{(1)}(t) = y^{(1)}(t)$ received by the AP. Notice that depending on the correlation matrix $\mathbf{R}$, optimal reception may require *joint* detection of the $L \times 1$ vector $\bar{\mathbf{s}}_{kn} := [s_{1kn}, \ldots, s_{Lkn}]^T$ containing the n^{th} symbol of the k^{th} user across the L clusters. The joint detector will rely on the $L \times 1$ decision vector $\mathbf{y}_{kn}^{(1)} := [y_{1kn}^{(1)}, \ldots, y_{Lkn}^{(1)}]^T$ whose components are given by

$$\begin{aligned} y_{lkn}^{(1)} &:= \int_{kn(T_s-1)}^{knT_s} y_{lk}^{(1)}(t) c_l(t - knT_s) dt \\ &= A \sum_{m=1}^{L} \rho_{ml} h_{mk} s_{mkn} + n_{lkn}^{(1)}. \end{aligned} \tag{28}$$

Upon defining $\mathbf{D}_k^{(1)} := \mathrm{diag}(h_{k1}, \ldots, h_{kL})$, we can rewrite (28) in matrix-vector form as

$$\mathbf{y}_{kn}^{(1)} = A \mathbf{R} \mathbf{D}_k^{(1)} \bar{\mathbf{s}}_{kn} + \mathbf{n}_{kn}^{(1)}, \quad k \in [1, K],\ n \in [1, N]. \tag{29}$$

The complexity of ML detection required to recover $\bar{\mathbf{s}}_{kn}$ from $\mathbf{y}_{kn}^{(1)}$ depends on the dimensionality L. While (29) models reception at the AP, a similar relationship characterizes reception in every cooperating user allowing U_{lk} to construct the estimate $\hat{\mathbf{s}}_{lk}$ of its cluster's aggregate block $\mathbf{s}_l$. Similar to Section II, we define $\mathcal{D}_l := \{U_{lk} \mid \hat{\mathbf{s}}_{lk} = \mathbf{s}_l\} \subseteq \mathcal{U}_l$; and let $h_{lk}^{(2)} = h_{lk}$ if $U_{lk} \in \mathcal{D}_l$, and $h_{lk}^{(2)} = 0$ else. As before, users $U_{lk} \in \mathcal{D}_l$ participate in phase-2.

Each cluster in phase-2 operates separately, repeating the steps described in Section II-B to construct $\mathbf{v}_l := [v_{l11}, \ldots, v_{l1N}, v_{l21}, \ldots, v_{lKN}]^T = \mathbf{\Pi}_2 \mathbf{\Phi} \mathbf{\Pi}_1 \mathbf{s}_l$ with $\mathbf{\Pi}_1$ and $\mathbf{\Pi}_2$ as in (19) and $\mathbf{\Phi} = \mathrm{diag}(\mathbf{\Theta}, \ldots, \mathbf{\Theta}) \in \mathbb{C}^{NK \times NK}$. Each user $U_{lk} \in \mathcal{D}_l$ then transmits the sub-block $\mathbf{v}_{lk} := [v_{lk1}, \ldots, v_{lkN}]^T$. Except for notation, these steps are identical to those in Section II-B. The difference is in the received signal which now comprises the superposition of waveforms transmitted from users in all L clusters

$$y_0^{(2)}(t) = A \sum_{l=1}^{L} \sum_{k=1}^{K} \sum_{n=1}^{N} v_{lkn} c_l[t - (N(k-1)+n)T_s] + n_0^{(2)}(t). \tag{30}$$

As in (28), we let $y_{lkn}^{(2)} := \int_{kn(T_s-1)}^{knT_s} y_0^{(2)}(t) c_l(t - knT_s) dt$ so that upon defining $\mathbf{y}_{kn}^{(2)} := [y_{1kn}^{(2)}, \ldots, y_{Lkn}^{(2)}]^T$, $\bar{\mathbf{v}}_{kn} := [v_{1kn}, \ldots, v_{Lkn}]^T$ and $\mathbf{D}_{0k}^{(2)} = \mathrm{diag}(h_{1k}^{(2)}, \ldots, h_{Lk}^{(2)})$, we can

[1]Although generalizations are immediate, to avoid further complication of the already heavy notation we will assume that the clusters have equal number of active users; i.e., $K_l = K$, $\forall l \in [1, L]$.

write $\mathbf{y}_{kn}^{(2)} = A\mathbf{R}\mathbf{D}_{0k}^{(2)}\bar{\mathbf{v}}_{kn} + \mathbf{n}_{kn}^{(2)}$, the counterpart of (29) for phase-2. For future use, it is convenient to define $\mathbf{y}_{0n}^{(2)} := [{\mathbf{y}^{(2)}}_{1n}^T, \ldots, {\mathbf{y}^{(2)}}_{Kn}^T]^T$, $\bar{\mathbf{v}}_n := [\bar{\mathbf{v}}_{1n}^T, \ldots, \bar{\mathbf{v}}_{Kn}^T]^T$, $\bar{\mathbf{R}} := \mathrm{diag}(\mathbf{R}, \ldots, \mathbf{R})$ and $\mathbf{D}_0^{(2)} := \mathrm{diag}(\mathbf{D}_{01}^{(2)}, \ldots, \mathbf{D}_{0K}^{(2)})$ and write

$$\mathbf{y}_{0n}^{(2)} = A\bar{\mathbf{R}}\mathbf{D}_0^{(2)}\bar{\mathbf{v}}_n + \mathbf{n}_{0n}^{(2)}. \tag{31}$$

On the other hand, let $\mathbf{u}_{ln} := [u_{l1n}, \ldots, u_{lKn}]^T$, $\mathbf{u}_n := [\mathbf{u}_{1n}^T, \ldots, \mathbf{u}_{Ln}^T]^T$ and $\mathbf{\Pi}_{LK} := [\mathbf{e}_1, \mathbf{e}_L, \ldots, \mathbf{e}_{(L-1)K+1}, \mathbf{e}_2, \mathbf{e}_{K+1}, \ldots, \mathbf{e}_{KL}]$ be a KL-dimensional periodic interleaver with period L. According to these definitions, we have $\bar{\mathbf{v}}_n = \mathbf{\Pi}_{LK}\mathbf{u}_n$. Also, note that since $\mathbf{u}_{ln} = \mathbf{\Theta}\mathbf{r}_{ln}$, for $\mathbf{r}_n := [\mathbf{r}_{1n}^T, \ldots, \mathbf{r}_{Ln}^T]^T$ and $\bar{\mathbf{\Phi}} = \mathrm{diag}(\mathbf{\Theta}, \ldots, \mathbf{\Theta}) \in \mathbb{C}^{LK\times LK}$, we have that

$$\mathbf{y}_{0n}^{(2)} = A\bar{\mathbf{R}}\mathbf{D}_0^{(2)}\mathbf{\Pi}_{LK}\bar{\mathbf{\Phi}}\mathbf{r}_n + \mathbf{n}_{0n}^{(2)}. \tag{32}$$

Concatenating (29) and (32) we obtain the ML decoder for $\mathbf{r}_n$ as

$$\hat{\mathbf{r}}_n = \arg\min_{\mathbf{r}_n\in\mathcal{S}^{LK}} \left\| \begin{bmatrix} \mathbf{y}_{0n}^{(1)} \\ \mathbf{y}_{0n}^{(2)} \end{bmatrix}_{2LK\times 1} - A \begin{bmatrix} \bar{\mathbf{R}}\mathbf{D}_0^{(1)} \\ \bar{\mathbf{R}}\mathbf{D}_0^{(2)}\mathbf{\Pi}_{LK}\bar{\mathbf{\Phi}} \end{bmatrix}_{2LK\times LK} \mathbf{r}_n \right\|. \tag{33}$$

Dimensionality of the multi-cluster ML decoder (33) is KL that has to be compared with K, the corresponding dimensionality of the ML decoder in (24) for the single-cluster case.

Even though the input-output relationships (29) and (32) as well as (3) and (8) model different systems they exhibit similar forms. An important consequence of this observation is that Corollary 3 establishing the diversity order of a single-cluster DCFC based MSC protocol can be readily generalized.

Corollary 4 *If $\mathbf{\Theta}$ is MDS with respect to $\mathcal{S}$, the multi-cluster DCFC based MSC protocol with the ML decoder in* (33) *achieves diversity equal to the number of users in each cluster; i.e.,*

$$\eta[\mathbf{\Pi}_2, \bar{\mathbf{\Phi}}, \mathbf{\Pi}_1, \mathbf{R}] = K. \tag{34}$$

Proof: For a Rayleigh channel, the coefficients h_{lk} are complex Gaussian and consequently the channel $\mathbf{D}_{0eq}^{(1)} := \bar{\mathbf{R}}\mathbf{D}_0^{(1)}$ is also Rayleigh. As in Corollary 3, notice from (31) that the diversity for Rayleigh distributed channel $\mathbf{D}_{0eq}^{(2)} := \bar{\mathbf{R}}\mathbf{D}_0^{(2)}$ is $\beta[\mathbf{\Pi}_2, \bar{\mathbf{\Phi}}, \mathbf{\Pi}_1, \mathbf{R}] = \min_{\bar{\mathbf{v}}_{n1}, \bar{\mathbf{v}}_{n2}} d_H(\bar{\mathbf{v}}_{n1}, \bar{\mathbf{v}}_{n2})$, [7, Sec. 2.1.2]. Since $\mathbf{\Pi}_{LK}$ is a permutation matrix, it follows that $d_H(\bar{\mathbf{v}}_{n1}, \bar{\mathbf{v}}_{n2}) = d_H(\bar{\mathbf{\Phi}}\mathbf{r}_{n1}, \bar{\mathbf{\Phi}}\mathbf{r}_{n2})$. The minimum d_H is achieved when all but one cluster transmit the same symbol block. Supposing without loss of generality that the first cluster transmits the distinct symbol block we have that $\mathbf{r}_{n1} := [\mathbf{r}_{1n}^T, \mathbf{r}_{2n}^T \ldots, \mathbf{r}_{Ln}^T]^T$ and $\mathbf{r}_{n2} := [\mathbf{r}_{1n2}^T, \mathbf{r}_{2n}^T \ldots, \mathbf{r}_{Ln}^T]^T$. The MDS property guarantees that for these $\mathbf{r}_{n1}, \mathbf{r}_{n2}$ selected, the minimum Hamming distance is $d_H(\bar{\mathbf{\Phi}}\mathbf{r}_{n1}, \bar{\mathbf{\Phi}}\mathbf{r}_{n2}) = K$. Invoking now Theorem 1, we deduce that $\eta[\mathbf{\Pi}_2, \bar{\mathbf{\Phi}}, \mathbf{\Pi}_1, \mathbf{R}] = \beta[\mathbf{\Pi}_2, \bar{\mathbf{\Phi}}, \mathbf{\Pi}_1, \mathbf{R}] = d_H(\bar{\mathbf{\Phi}}\mathbf{r}_{n1}, \bar{\mathbf{\Phi}}\mathbf{r}_{n2}) = K$. □

As expected, Corollary 4 proves that the diversity enabled by DCFC remains invariant regardless of the structure of the correlation matrix $\mathbf{R}$.

Remark 3 For clarity, we have considered MA in fixed cooperative networks. However, the same scheme and results are also valid for ad-hoc networks. In this case, different sources per cluster cooperate while communicating with (possibly) different destinations. Different clusters operate without coordination.

A. Effect of under-spreading in spectral efficiency

Consider a set of orthonormal functions $\mathcal{N} := \{\nu_s(t)\}_{s=1}^S$ with $\int_0^{T_s} \nu_{s_1}(t)\nu_{s_2}(t)dt = \delta(s_1 - s_2)$, where $\delta(\cdot)$ denotes Kronecker's delta. It is customary to write the signature waveforms in (26) as the linear combination

$$c_l(t) = \sum_{s=1}^{S} c_{ls}\nu_s(t), \qquad t \in [0, T_s),\ l \in [1, L], \tag{35}$$

where the vector $\mathbf{c}_l := [c_{l1}, \ldots, c_{lS}]^T$ is the spreading code specific to the cluster $\mathcal{U}_l$. Arranging the codes in a matrix $\mathbf{C} := [\mathbf{c}_1, \ldots, \mathbf{c}_L]$ we can write the correlation matrix as $\mathbf{R} = \mathbf{C}^{\mathcal{H}}\mathbf{C}$. Changing the set $\mathcal{N}$ we can model different CDMA systems; if the functions are delayed versions of each other $\nu_s(t) = p[St-(s-1)T_s)]$, then (35) amounts to symbol-periodic direct sequence (DS)-CDMA; if they are different subcarriers, $\nu_s(t) = \exp[j2\pi(s-1)t/T_s]p(t)$, then (35) models multi-carrier (MC)-CDMA.

Transmission of $\nu_s(t)$ requires S times more bandwidth than transmission of the pulses $p(t)$ in (2). Consequently, the spectral efficiency of multi-cluster DCFC is

$$\xi = L/(2S). \tag{36}$$

An important choice in the selection of $\mathbf{C}$ is whether the spreading gain S constrains *a fortiori* the number of codes L or not. This calls for distinguishing between *under-spread* and *over-spread* MA:

Definition 2 *In an over-spread MA system, the number of codes L and the spreading gain S are constrained by $S \geq L$. We say that an MA system is under-spread if L and S can be selected independently.*

Over-spread orthonormal MA: In this case, $\mathbf{C}$ is formed by orthonormal vectors, e.g., Walsh-Hadamard sequences, so that $\mathbf{R} := \mathbf{C}^{\mathcal{H}}\mathbf{C} = \mathbf{I}_L$. But the latter requires $L \leq S$ because a set of orthonormal vectors in $\mathbb{C}^S$ cannot contain more than S elements. Thus, orthonormal MA is over-spread in the sense of Definition 2.

Under-spread MA: Symbol-periodic non-orthogonal signatures, including those in MC-CDMA and DS-CDMA with Gold or Kasami sequences [3], implement under-spread MA since L can be much larger than S. Long pseudo-noise (PN) sequences also give rise to under-spread MA with approximately uncorrelated signatures. Since the latter can be theoretically infinite, L and S are decoupled and long code DS- or MC-CDMA is also under-spread in the sense of Definition 2.

Since in orthonormal MA, clusters do not interfere with each other, the multi-cluster model in (33) can be reduced to a set of single-cluster models (24). Thus, the ML decoding space dimension is reduced from KL to K. PN sequences, on the other hand, have found widespread use due to their robustness to propagation delays and relaxed synchronization

TABLE I
COMPARISON OF DIFFERENT PROTOCOLS

	Performance metrics	Repetition coding	Distributed ECC	DCFC	Non-cooperative
over-spread MA	diversity (η)	2	$\min(d_{\min}, \lfloor 1 + K(1-R_c) \rfloor)$	K	1
	spectral eff. (ξ)	$1/2$	$1/2$	$1/2$	1
	complexity	1	KN	K	1
under-spread MA	diversity (η)	2	$\min(d_{\min}, \lfloor 1 + K(1-R_c) \rfloor)$	K	1
	spectral eff. (ξ)	1	1	1	1
	complexity	L	LKN	LK	1

requirements. The decision as to whether to use under- or over-spread MA may also depend on other factors as well.

MSC protocols with under-spread versus over-spread MA are fundamentally different in terms of bandwidth efficiency. In over-spread MA the spectral efficiency of MSC protocols is hard limited by $\xi_{\rm MSC} \leq 1/2$ [c.f. (36) and Definition 2] and cooperation comes at the price of reducing the spectral efficiency $\xi_{\rm NC} = 1$ of the corresponding non-cooperative system. In e.g., orthonormal MA, this is because $L \leq S$ clusters can have orthogonal signatures. In under-spread MA, bandwidth efficiency and cooperative diversity are not necessarily traded off since L and S are decoupled. Indeed, we can obtain $\xi_{\rm MSC} = \xi_{NC}$ by reducing the spreading gain by half, i.e., $S_{\rm MSC} = S_{NC}/2$ while maintaining the same number of clusters L [c.f. (36)]. Note that even if we reduce the spreading gain by half, after completing both MSC phases each information symbol has been transmitted twice and the effective coding gain is still the same as in non-cooperative MA. Nonetheless, a consequence of Corollary 4 is that the diversity gain is $\eta[\mathbf{\Pi}_2, \bar{\mathbf{\Phi}}, \mathbf{\Pi}_1, \mathbf{R}] = K$, regardless of the correlation structure $\mathbf{R}$. Thus, under-spread MA with DCFC *achieves full diversity* without sacrificing spectral efficiency.

IV. COMPARING MSC WITH NON-COOPERATIVE PROTOCOLS

So far, we have considered three different MSC protocols, namely distributed repetition coding, distributed ECC and DCFC defined in [C1], [C2] and [C3], respectively. We also distinguished between under- and over-spreading for cluster separation as per Definition 2, for a total of six different alternatives. These alternatives differ in their diversity η [c.f. (1)], spectral efficiency ξ [c.f. (36)] and decoding complexity as we summarize in Table I.

Repetition coding can afford the lowest decoding complexity, but also enables the smallest diversity order. Moreover, the diversity order it enables is independent of the number of users in the cluster. The diversity order can be increased with either distributed ECC or DCFC at the expense of increasing decoding complexity. It is known that $\eta \approx 4$ brings the wireless channel within a 10% of an AWGN channel's error performance [18], meaning that $K \approx 4$ captures enough of the diversity advantage. Thus, a slight complexity increase brings in a substantial error performance gain. This is particularly true for DCFC that achieves full; i.e., $\eta = K$, diversity. For distributed ECC a larger cluster is possibly needed.

Under- and over-spreading are fundamentally different in terms of bandwidth efficiency ξ. In the rows corresponding to over-spread MA, ξ is reduced from 1 to $1/2$ for any of the MSC protocols. The value of ξ in the corresponding columns of Table I for under-spread MA is not affected when we move from non-cooperative MA to MSC. The value $\xi = 1$ is an arbitrary selection and should be interpreted as an option to allow for a fair comparison between over-spread non-cooperative MA and under-spread cooperative MA. Interestingly, the use of under-spread MA with DCFC achieves full diversity K while avoiding the bandwidth penalty usually associated with cooperative protocols as we can see by comparing the second with the fifth row of Table I.

All in all, in a complexity-limited system repetition coding offers the best MSC protocol, while in a bandwidth-limited setup DCFC-based MSC with under-spreading for cluster separation should be preferred. In intermediate cases, DCFC-based MSC with (over-spread) orthonormal cluster separation achieves full diversity with reasonable spectral-efficiency ($\xi = 1/2$) and a modest increase in complexity.

V. SIMULATIONS

In this section, we present simulated examples to corroborate our analytical claims. Each user transmits blocks with $N = 50$ symbols per TDMA slot. Except for one example, we assume error-free channels between users. We choose the CFC encoder $\mathbf{\Theta}$ to be the unitary Vandermonde matrix in [19]

$$\mathbf{\Theta} = \frac{1}{\sqrt{K}} \mathbf{F}_K^H \text{diag}(1, \alpha, \ldots, \alpha^{K-1}), \tag{37}$$

where $\mathbf{F}_K$ is the $K \times K$ fast Fourier transform (FFT) matrix with (i,j)th entry $[\mathbf{F}_K]_{ij} := e^{-j2\pi(i-1)(j-1)/K}$; and $\alpha := e^{j\pi/(2K)}$ if K is power of 2, $\alpha := e^{j\pi/9}$ if $K = 3$, and $\alpha := e^{j\pi/25}$ if $K = 5$.

A. DCFC based MSC with orthonormal MA

Consider first the DCFC based MSC protocol with orthonormal CDMA signatures used for cluster separation. According to Table I, the ML decoder operates on blocks of length K, the spectral efficiency is $\xi = 1/2$ and the diversity order is $\eta = K$. To benchmark performance consider error-free links between users, in which case $\mathcal{D} \equiv \mathcal{U}$. Fig. 5 demonstrates how the bit error rate (BER) varies with K for a DCFC based MSC protocol. We verify that the diversity order is, indeed, equal to the number of users K. For reference, we also depict the BER of a non-cooperative system and repetition based MSC [14]. For $K = 2$ repetition based MSC outperforms DCFC based MSC by a small margin. This is because in this case both protocols have the same diversity gain but the coding gain of DFCF is smaller. The advantage of DCFC is apparent for larger cooperating clusters. Setting e.g., $K = 5$, we can see

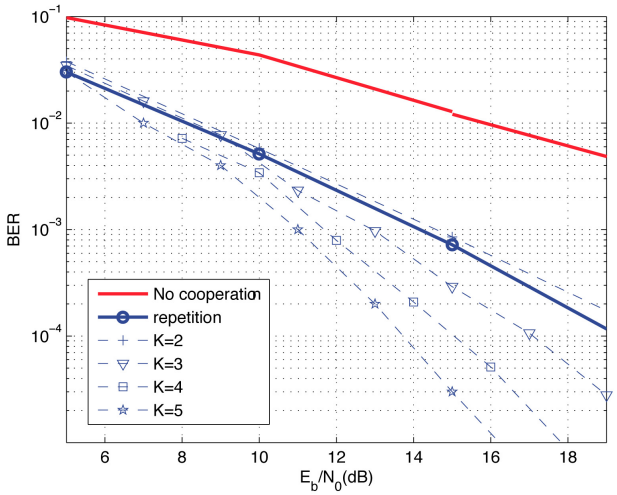

Fig. 5. BER of orthonormal DCFC-based MSC with variable number of users, and error-free user-to-user links.

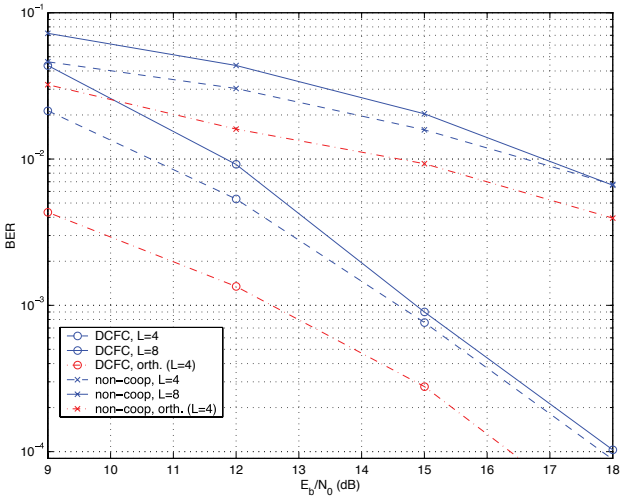

Fig. 7. BER of under-spread DCFC-based MSC with different values of spectral efficiency.

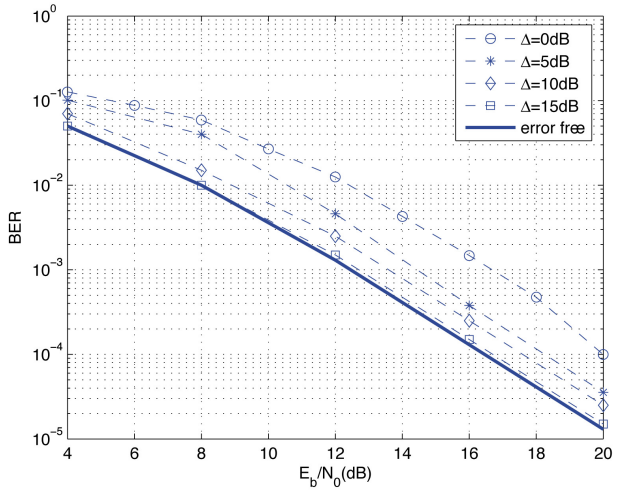

Fig. 6. BER of orthonormal DCFC-based MSC with variable relative SNRs in the links between user pairs.

that with a minimal investment in decoding complexity, DCFC based MSC returns a $4-5$ dB gain with respect to repetition based MSC due to the increase in diversity from $\eta = 2$ to $\eta = K = 5$.

Even though the simulated curves in Fig. 5 are for error-free user-to-user links, the same results are obtained when we account for the effect of decoding errors in these links as verified by Fig. 6 for $K = 3$. We consider different values of the relative SNR $\Delta := \gamma_{k,j}/\gamma_k = \mathrm{E}[h_{k,j}^2]/\mathrm{E}[h_k^2]$, where we recall $\gamma_{k,j}$ is the average SNR of the $U_k \to U_j$ link and γ_k is the average SNR in the $U_k \to$AP link. Regardless of Δ, the diversity order is always $\eta = K = 3$ as asserted by Theorem 1, but the coding gain changes, as predicted. Notwithstanding, the gap between error-free $U_k \to U_j$ links and $\Delta = 5$dB is approximately 2dB, and reduces to less than 1dB for $\Delta = 10$dB. Thus, in many practical settings proximity of cooperators ensures that MSC protocols work almost as well as non-cooperative single-user multi-antenna systems.

B. DCFC based MSC with under-spread MA

Spectral efficiency in the simulated systems of the previous subsection is $\xi = 1/2$. This is not the case for DCFC with under-spread MA which according to Table I requires ML decoding on blocks of length KL, but attains spectral efficiency $\xi = 1$ and diversity order $\eta = K$. In Fig. 7 we show BER for $K = 3$, $S = 8$ and $L = 4$ – $L = 8$ with PN codes used to implement under-spread cluster separation. Verifying Corollary 4, the diversity order is $\eta = K = 3$ regardless of the number of clusters L. When $L = 8$ the spectral efficiency is $\xi = 1$ and it is pertinent to compare DCFC with a non-cooperative protocol with orthonormal MA (for which $\xi = 1$ too). The diversity enabled by DCFC leads to a considerable BER reduction. When $L = 4$ the spectral efficiency is $\xi = 1/2$. In this case, it is possible to use DCFC based MSC with orthonormal MA. We can see that gaining in spectral efficiency with DCFC entails a loss in coding gain of about 2dB. Interestingly, the coding gain is affected by the use of under-spread MA but the diversity order is not. Complexity allowing, DCFC based MSC with under-spread MA is the choice for bandwidth-limited scenarios, whereas if bandwidth is plenty the use of orthonormal MA should be preferred for its larger coding gain.

C. DCFC versus Distributed ECC

Even though we established that the diversity order of DCFC is in general larger than the diversity of distributed (D)ECC in [C2] (see Table I), the latter has in general a larger coding gain. To demonstrate these differences, we consider clusters with $K = 3$ users and compare DCFC based MSC against MSC based on distributed convolutional coding (DCC) with rate $1/2$ and generator in octal form $[15/7]$. The free distance of this code is $d_{\min} = 5$ and consequently the diversity order is $\eta_{DCC} = 2$. The interleavers Π_1, Π_2 are designed as in [17] to ensure that this diversity is actually achieved.

Fig. 8 illustrates that due to its larger diversity order DCFC outperforms DCC at high SNR while the opposite is true

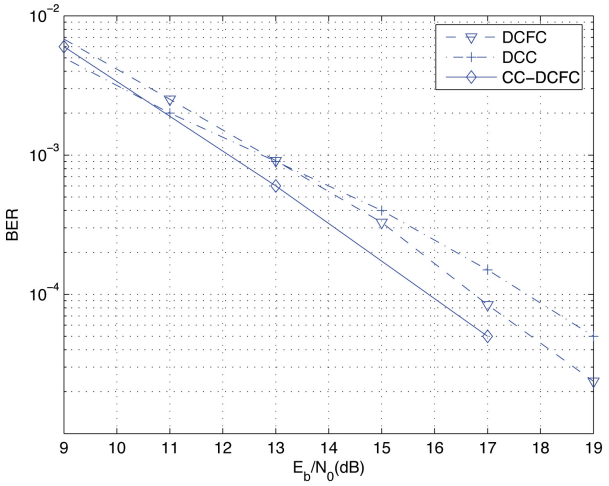

Fig. 8. BER of orthonormal DCFC and DCC based MSC protocols.

at low SNR due to the larger coding gain of DCC based MSC. We can also use CC and DCFC together to jointly exploit the coding gain of CC and the diversity order of DCFC. This is done by encoding each user's bits with a CC *before* transmitting $\mathbf{s}_k$. At the receiver, we adopt soft iterative decoding between CC and DCFC decoders along the lines of [19]. As depicted in Fig. 8, there is about 1dB gain achieved with a CC of memory 2. Another advantage of DCFC is that the interleavers are simple periodic multiplexers as opposed to carefully designed interleavers needed for DCC in [17].

VI. Conclusions

We introduced a general multi-source cooperation (MSC) framework for multi-cluster networks that allows flexible tradeoffs between error performance, spectral efficiency and complexity. Our MSC protocols rely on code division multiple access (CDMA) for cluster separation and time division multiple access (TDMA) for user separation per cluster. The unifying framework includes many existing protocols as particular cases and suggests the introduction of distributed complex field coding (DCFC) to enable diversity as high as the number of per-cluster users. We also demonstrated the different spectral efficiency properties of over-spread, e.g., orthonormal, and under-spread, e.g., MC-CDMA or DS-CDMA with Gold or Kasami sequences, cluster separation. Whereas in the former cooperative diversity is traded off for bandwidth in the latter there is no bandwidth penalty associated with user cooperation.

Adjusting the number of cooperating users, MSC encoder, spreading gain and/or number of clusters, our general MSC framework is flexible to tradeoff among spectral-efficiency, decoding complexity and diversity. By increasing complexity, the combination of DCFC with under-spread multiple access enables high order diversity with spectral efficiency up to that of non-cooperative systems. In cases where bandwidth is not the limiting resource, DCFC-based MSC with over-spread orthonormal cluster separation allows one to collect full diversity with reasonable spectral-efficiency and a modest increase in complexity[2].

Appendices

A. Proof of Lemma 1: Let $\delta(\mathbf{f};\mathbf{g})$ be the indicator function of $\mathbf{f} \neq \mathbf{g}$ taking on the values $\delta(\mathbf{f};\mathbf{g}) = 1$ if $\mathbf{f} \neq \mathbf{g}$ and $\delta(\mathbf{f};\mathbf{g}) = 0$ if $\mathbf{f} = \mathbf{g}$; and consider two distinct codewords $[\mathbf{s}^T, \mathbf{v}^T] = [\mathbf{s}_1^T, \ldots, \mathbf{s}_K^T, \mathbf{v}_1^T, \ldots, \mathbf{v}_K^T]$ and $[\tilde{\mathbf{s}}^T, \tilde{\mathbf{v}}^T] = [\tilde{\mathbf{s}}_1^T, \ldots, \tilde{\mathbf{s}}_K^T, \tilde{\mathbf{v}}_1^T, \ldots, \tilde{\mathbf{v}}_K^T]$. If $\mathcal{D} = \mathcal{U}$, then MSC is equivalent to a multi-antenna channel, in which case the diversity achieved depends on the triplet $(\mathbf{\Pi}_2, \psi(\cdot), \mathbf{\Pi}_1)$. If we define $\beta(\mathbf{s};\tilde{\mathbf{s}})$ as the pairwise error probability (PEP) diversity order we have [2]

$$\begin{aligned}\beta(\mathbf{s};\tilde{\mathbf{s}}) &:= -\lim_{\gamma\to\infty} \frac{\log\left[\Pr(\mathbf{s}\to\tilde{\mathbf{s}}|\mathcal{D}=\mathcal{U})\right]}{\log(\gamma)} \\ &= \sum_{k=1}^{K} \delta\left([\mathbf{s}_k^T, \mathbf{v}_k^T]; [\tilde{\mathbf{s}}_k^T, \tilde{\mathbf{v}}_k^T]\right). \end{aligned} \tag{38}$$

That is, the probability that we declare $\tilde{\mathbf{s}}$ when the actual transmitted block is $\mathbf{s}$ goes to zero as $\gamma^{-\beta(\mathbf{s};\tilde{\mathbf{s}})}$, with $\beta(\mathbf{s};\tilde{\mathbf{s}})$ given by (38). Consequently, if $[\mathbf{s}_k^T, \mathbf{v}_k^T] = [\tilde{\mathbf{s}}_k^T, \tilde{\mathbf{v}}_k^T]$ user U_k does not contribute to the diversity order of this particular pair and if $[\mathbf{s}_k^T, \mathbf{v}_k^T] \neq [\tilde{\mathbf{s}}_k^T, \tilde{\mathbf{v}}_k^T]$ U_k contributes one unit to the PEP exponent in (38).

If $U_k \notin \mathcal{D}$ then $h_k^{(2)} = 0$, which is equivalent to having $\mathbf{v}_k$ and $\tilde{\mathbf{v}}_k$ punctured. Thus, each $U_k \notin \mathcal{D}$ reduces $\beta(\mathbf{s};\tilde{\mathbf{s}})$ by (at most) 1 which implies that the PEP diversity order conditioned on $\mathcal{D}$ is bounded as

$$\begin{aligned}\eta(\mathbf{s};\tilde{\mathbf{s}}|\mathcal{D}) &:= -\lim_{\gamma\to\infty} \frac{\log\left[\Pr(\mathbf{s}\to\tilde{\mathbf{s}}|\mathcal{D})\right]}{\log(\gamma)} \\ &= \sum_{k|U_k\in\mathcal{D}} \delta\left([\mathbf{s}_k^T, \mathbf{v}_k^T]; [\tilde{\mathbf{s}}_k^T, \tilde{\mathbf{v}}_k^T]\right) \\ &\geq \max[0; \beta(\mathbf{s};\tilde{\mathbf{s}}) - (K - |\mathcal{D}|)]. \end{aligned} \tag{39}$$

Finally, note that $\beta = \min_{\mathbf{s};\tilde{\mathbf{s}}} \beta(\mathbf{s};\tilde{\mathbf{s}})$ and likewise for $\eta(\mathcal{D})$. But if (38) holds for any pair of codewords it must hold for their minima and (13) follows. □

B. Proof of Lemma 2: Let $F(k,j) := \{\hat{\mathbf{s}}_{k,j} \neq \mathbf{s}_j\}$ denote the event that U_k fails to correctly decode U_j's message. The probability of $F(k,j)$ can be obtained by averaging over the realizations of $h_{k,j}$ to obtain

$$\begin{aligned}\Pr\{F(k,j)\} &= \mathrm{E}_{h_{k,j}}[\Pr\{F(k,j)|h_{k,j}\})] \\ &= \mathrm{E}_{h_{k,j}}\left[1 - \left(1 - Q\left(\sqrt{\kappa\gamma|h_{k,j}|^2}\right)\right)^N\right], \end{aligned} \tag{40}$$

where $\gamma|h_{k,j}|^2$ is the instantaneous SNR in the $U_i \to U_j$ link, N is the length of the symbol vector from one user, and κ is a constant dependent on the constellation. It is not difficult to

[2] The views and conclusions contained in this document are those of the authors and should not be interpreted as representing the official policies, either expressed or implied, of the Army Research Laboratory or the U. S. Government.

show that as γ increases we have, see e.g., [9, Chap. 14]

$$\lim_{\gamma\to\infty} \frac{\log\left[\Pr\{F(k,j)\}\right]}{\log(\gamma)} = \lim_{\gamma\to\infty} \frac{\log\left[\mathrm{E}_{h_{k,j}}\left(NQ\left(\sqrt{\kappa\gamma|h_{k,j}|^2}\right)\right)\right]}{\log(\gamma)} = -1. \tag{41}$$

Since the events $F(k,j)$ are independent, the probability of a given user being part of $\mathcal{D}$ is such that

$$\Pr(U_k \notin \mathcal{D}) \leq \Pr\left(\bigcup_{j=1,j\neq k}^{K} F(k,j)\right) = \sum_{j=1,j\neq k}^{K} \Pr\left(F(k,j)\right). \tag{42}$$

But since (41) is valid for all $F(k,j)$ we have that [c.f. (41), (42)]

$$\lim_{\gamma\to\infty} \frac{\log\left[\Pr(U_k \notin \mathcal{D})\right]}{\log(\gamma)} \leq \lim_{\gamma\to\infty} \frac{\log\left[\sum_{j=1,j\neq k}^{K} \Pr\left(F(k,j)\right)\right]}{\log(\gamma)} = -1. \tag{43}$$

On the other hand, the probability of $\mathcal{D}$ can be bounded as

$$\Pr(\mathcal{D}) = \prod_{U_k\notin\mathcal{D}} \Pr(U_k \notin \mathcal{D}) \prod_{U_k\in\mathcal{D}} \Pr(U_k \in \mathcal{D}) \leq \prod_{U_k\notin\mathcal{D}} \Pr(U_k \notin \mathcal{D}), \tag{44}$$

where the inequality follows since $\Pr(U_k \in \mathcal{D}) \leq 1$. Using (44) we can finally write for the limit in (14)

$$\lim_{\gamma\to\infty} \frac{\log\left[\Pr(\mathcal{D})\right]}{\log(\gamma)} = \sum_{U_k\notin\mathcal{D}} \lim_{\gamma\to\infty} \frac{\log\left[\Pr(U_k \notin \mathcal{D})\right]}{\log(\gamma)}. \tag{45}$$

Since the sum in (45) contains $K - |\mathcal{D}|$ elements, (14) follows after substituting (43) into (45). □

REFERENCES

[1] K. Azarian, H. El Gamal, and P. Schniter, "On the achievable diversity-multiplexing tradeoff in half-duplex cooperative channels," *IEEE Transactions on Information Theory*, 2006 (to appear).

[2] M. Chiani, A. Conti, and V. Tralli, "Further results on convolutional code search for block-fading channels," *IEEE Trans. Inform. Theory*, vol. 50 , no. 6, pp. 1312–1318, June 2004.

[3] E. Dinan and B. Jabbari, "Spreading codes for direct sequence CDMA and wideband CDMA cellular networks," *IEEE Communications Magazine*, vol. 36, pp. 48–54, Sept. 1998.

[4] B. Hassibi and H. Vikalo, "On the expected complexity of sphere decoding," in *Proc. of 35th Asilomar Conf. on Signals, Systems, and Computers*, Pacific Grove, CA, pp. 1051–1055, Nov. 2001.

[5] M. Janani, A. Hedayat, T. Hunter, and A. Nosratinia, "Coded cooperation in wireless communications: space-time transmission and iterative decoding," *IEEE Trans. on Signal Processing*, vol. 52, pp. 362–371, Feb. 2004.

[6] J. N. Laneman and G. W. Wornell, "Distributed Space-Time Coded Protocols for Exploiting Cooperative Diversity in Wireless Networks," *IEEE Trans. on Information Theory*, vol. 49, pp. 2415–2425, Oct. 2003.

[7] X. Ma and G. B. Giannakis, "Complex field coded MIMO systems: performance, rate, and trade-offs," *Wireless Communications and Mobile Computing*, vol. 2, pp. 693–717, Nov. 2002.

[8] M. Pohst, "On the computation of lattice vectors of minimal length, successive minima and reduced bases with applications," in *ACM SIGSAM*, pp. 37–44, 1981.

[9] J. G. Proakis, *Digital communications*. New York: McGraw Hill, 4th ed. ed., 1995.

[10] A. Ribeiro, R. Wang, and G. Giannakis, "Multi-source cooperation with full-diversity spectral-efficiency and controllable-complexity," in *IEEE Workshop on Signal Proc. Advances in Wireless Comm.*, Cannes, France, July 2-5, 2006 (to appear).

[11] A. Ribeiro, X. Cai, and G. B. Giannakis, "Opportunistic multipath for bandwidth-efficient cooperative networking," in *Proc. of the International Conference on Acoustics Speech and Signal Processing*, vol. 4, pp. 549–552, Montreal, Canada, May 2004.

[12] G. Scutari and S. Barbarossa, "Distributed space-time coding for regenerative relay networks," *IEEE Transactions on Wireless Communications*, vol. 4, pp. 2387–2399, Sept. 2005.

[13] G. Scutari, S. Barbarossa, and D. Ludovici, "Cooperation diversity in multihop wireless networks using opportunistic driven multiple access," in *4th IEEE Workshop on Signal Proc. Advances in Wireless Comm.*, Rome, Italy, pp. 170 – 174, 15-18 June 2003.

[14] A. Sendonaris, E. Erkip, and B. Aazhang, "User cooperation diversity," *IEEE Trans. Commun.*, vol. 51, pp. 1927–1948, Nov. 2003.

[15] O. Shalvi, "Multiple Source Cooperation Diversity," *IEEE Communication Letters*, vol. 8, No. 12, pp. 712–714, Dec. 2004.

[16] R. Wang, W. Zhao, and G. B. Giannakis, "Distributed Trellis Coded Modulation for Multi-Source Cooperative Networks," in *Proc. of the IEEE Radio Wireless Symposium*, San Diego, CA, Jan. 17-19, 2006.

[17] R. Wang, W. Zhao, and G. B. Giannakis, "Multi-Source Cooperative Networks with Distributed Convolutional Coding," in *39th Annual Asilomar Conference on Signals, Systems, and Computers*, Pacific Grove, CA, Oct. 30-Nov. 2, 2005.

[18] Z. Wang, S. Zhou, and G. Giannakis, "Joint coding-precoding with low-complexity turbo-decoding," *IEEE Trans. on Wireless Communications*, vol. 3, no. 3, pp. 832–842, May 2004.

[19] Y. Xin, Z. Wang, and G. B. Giannakis, "Space-Time Diversity Systems based on Linear Constellation Precoding," *IEEE Trans. on Wireless Communications*, vol. 2, no. 2, pp. 294–309, March 2003.

[20] W. Zhao and G. Giannakis, "Reduced complexity closest point decoding algorithms for random lattices," *IEEE Transactions on Wireless Communications*, vol. 5, no. 1, pp. 101–111, January 2006.

Alejandro Ribeiro received his B.Sc. degree in Electrical Engineering from Universidad de la Republica Oriental del Uruguay, Montevideo, Uruguay in 1998. Since May 2003 he has been working towards his Ph.D. degree in the Department of Electrical and Computer Engineering, University of Minnesota, Minneapolis, MN where he received his M.Sc. degree in Electrical Engineering in 2005.

From 1998 to 2003 he was a member of the Technical Staff at Bellsouth Montevideo. His research interests lie in the areas of communication theory, signal processing and networking. His current research focuses on wireless cooperative communications, random access, wireless ad hoc and sensor networks, and distributed signal processing. Mr. Ribeiro is a Fulbright Scholar.

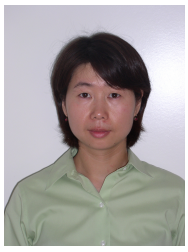

Renqiu Wang received her B.S. degree in electrical engineering and information science from the University of Science and Technology of China (USTC) in 1998, and the M.Sc. degree and Ph.D. in electrical engineering from the University of Minnesota, Minneapolis, MN, in 2003 and 2006 respectively. From 1998 to 2001, she worked for the Shanghai Bell Company, China, on switching networks and the third generation mobile communication systems. Her research interests include signal processing applications in communications, spacetime processing and coding, turbo decoding algorithms and cooperative networks.

Georgios B. Giannakis (F'97) received his Diploma in Electrical Engineering from the National Technical University of Athens, Greece, 1981. From September 1982 to July 1986 he was with the University of Southern California (USC), where he received his MSc. in Electrical Engineering, 1983, MSc. in Mathematics, 1986, and Ph.D. in Electrical Engineering, 1986. After lecturing for one year at USC, he joined the University of Virginia in 1987, where he became a professor of Electrical Engineering in 1997. Since 1999 he has been a professor with the Department of Electrical and Computer Engineering at the University of Minnesota, where he now holds an ADC Chair in Wireless Telecommunications.

His general interests span the areas of communications and signal processing, estimation and detection theory, time-series analysis, and system identification – subjects on which he has published more than 250 journal papers, 400 conference papers and two edited books. Current research focuses on diversity techniques for fading channels, complex-field and space-time coding, multicarrier, ultra-wide band wireless communication systems, cross-layer designs and sensor networks.

G. B. Giannakis is the (co-) recipient of six paper awards from the IEEE Signal Processing (SP) and Communications Societies (1992, 1998, 2000, 2001, 2003, 2004). He also received Technical Achievement Awards from the SP Society in 2000 and from EURASIP in 2005. He served as Editor in Chief for the *IEEE SP Letters*, as Associate Editor for the *IEEE Trans. on Signal Proc.* and the *IEEE SP Letters*, as secretary of the SP Conference Board, as member of the SP Publications Board, as member and vice-chair of the Statistical Signal and Array Processing Technical Committee, as chair of the SP for Communications Technical Committee and as a member of the IEEE Fellows Election Committee. He has also served as a member of the IEEE-SP Society's Board of Governors, the Editorial Board for the *Proceedings of the IEEE* and the steering committee of the *IEEE Trans. on Wireless Communications*.